

Adapted Tx-SENSE excitation to account for inhomogeneous slice refocusing at 7T

T. D. Lindel^{1,2}, F. Seifert^{1,2}, M. Dietterle^{1,2}, T. Niendorf², and B. Ittermann^{1,2}

¹Physikalisch-Technische Bundesanstalt, Braunschweig und Berlin, Germany, ²Berlin Ultrahigh Field Facility, Max-Delbrück-Centrum für Molekulare Medizin, Berlin, Germany

Introduction: Parallel transmission (pTx) is frequently used to address B_1^+ inhomogeneity issues at ultrahigh magnetic fields [1,2]. pTx comes in three major flavors: B_1 shimming [3], spokes excitation [4], and Tx-SENSE [5]. The latter technique is the most powerful approach allowing not just B_1^+ homogenization but also spatially selective excitation (SSE); its applicability, however, is hitherto still very limited. First results on 3D-SSE exist [6,7] but are not yet available for the case of clinical scanners at $B_0 \geq 7$ T, where wave effects and B_1^+ distortions are most severe. 2D-Tx-SENSE pulses are well established for planar SSE but excite the whole object in the normal direction. They have to be combined with a (conventional) slice selective refocusing pulse in order to restrict the field of excitation (FOX) in the third dimension. In this paper we investigate the effect of this refocusing pulse on the quality of SSE images.

Methods: All experiments were performed on a clinical 7-T scanner (Siemens Healthcare, Erlangen) equipped with an 8-channel Tx array. An 8-channel Tx/Rx head coil (Rapid Biomedical, Rimpax) was used to image a cylindrical agarose gel phantom (0.66 g/l CuSO_4 , 1.33 g/l NaCl, i.d.=19cm, l=20 cm). Tx-SENSE pulses were calculated similarly as described in [8]. Excitation k -space was traversed at constant slew rate in a 32-turn spiral using 4-fold acceleration and 2.5-ms RF pulses; a conventional 6-ms sinc pulse with nominally 180° flip angle was used for refocusing. The target pattern for SSE was a homogeneous $81 \times 81 \text{ mm}^2$ square with apodized profile to avoid excitation ringing artifacts. Without refocusing such a pattern could be excited with about 10% residual background outside and about 10% signal variation inside the target region [9].

Results: In Fig 1a) a conventional low-flip angle GRE image with the coil driven in CP mode is shown together with intensity profiles along four different cuts. The image reflects the inhomogeneities of the refocusing pulse; features like the ring of almost vanishing B_1^+ are well known for water-like phantoms in ultrahigh-field MRI. Refocusing with such a pulse after homogeneous 2D-SSE results in severe distortions as it transfers the CP inhomogeneity to the image (Fig 1b). To improve this situation we applied B_1 shimming of the echo pulse: amplitudes and phases of each transmit channel were optimized for best B_1^+ homogeneity in the target region. B_1 shimming is not strong enough to ensure signal homogeneity over the whole phantom but is capable to remove the most severe distortions from the region of interest (Fig 1c), thus considerably improving the SSE result (Fig 1d). Nevertheless we end up with unsatisfactory $\sim 30\%$ signal variation over the target area. However, based on the known B_1^+ maps for each coil element the B_1 shimming efficacy and residual distortion due to the refocusing pulse can be determined in advance. By pre-distorting the target pattern correspondingly, adapted 2D-SSE pulses were calculated anticipating and compensating the imperfections of the subsequent refocusing. With this approach we achieve excellent definition of the target pattern, good background suppression, and flat profiles along any direction (Fig. 2a). A high resolution zoomed image (Fig. 2b) also exhibits almost perfect flatness of the target pattern.

Conclusion: We demonstrated the need for and the feasibility of corrective measures if 2D-SSE is to be combined with a conventional (even B_1 shimmed) slice selective refocusing pulse. The proposed adaptation step can easily be implemented into any existing SSE pulse calculation algorithm and improves image quality considerably whenever full 3D-SSE pulses are not available or not applicable.

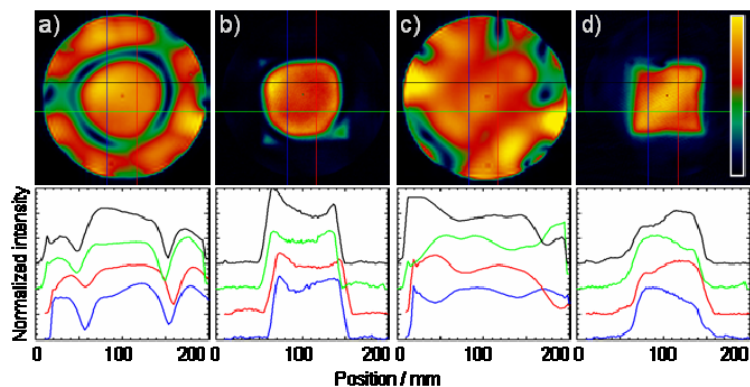


Fig. 1 a): Low flip angle GRE image after CP mode excitation and normalized 1D profiles along 4 different cuts underneath. b): 2D-SSE with CP refocusing, $\text{FOX}=(81\text{mm})^2$. c): GRE image with B_1 shimming optimized for homogeneity in the indicated target region. d): 2D-SSE with B_1 shimmed refocusing. a-d): Tx/Rx matrices $32^2/128^2$; $\text{FOV}=(20\text{cm})^2$; all data normalized to phantom-center intensity; 1D-profiles vertically offset for clarity; color scale indicated in d).

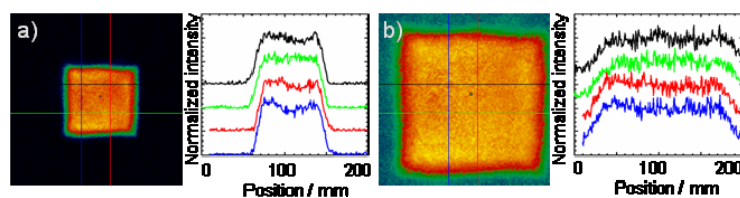


Fig. 2 a): Adapted 2D-SSE and B_1 shimmed refocusing. Tx/Rx matrices $64^2/256^2$, $\text{FOX}/\text{FOV}=(81/200\text{mm})^2$. b): High resolution zoomed image; Tx/Rx matrices $64^2/512^2$; $\text{FOX}/\text{FOV}=(81/100\text{mm})^2$, kernel smoothing (1.1 mm) for noise reduction.

References and Acknowledgement: [1] Wu X et al., MRM 63 (2010) 524. [2] Setsompop K et al., J Magn Reson 195 (2008) 76. [3] Seifert F et al., JMRI 26 (2007) 1315. [4] Saekho S et al., MRM 55 (2006) 719. [5] Katscher U et al., MRM 49 (2003) 144. [6] Schneider JT et al., Proc. ISMRM 2010, 103. [7] Vahedipour K et al., Proc. ISMRM 2010, 4917. [8] Grissom W et al., MRM 56 (2006) 620. [9] Seifert F et al, MAGMA 22 Suppl 1 (2009) 256. This work was supported by the INUMAC project under BMBF grant #13N9207.